Mesocirculation Associated with Summer Convection over the Central Antilles

Mark R. Jury*

Physics Department, University of Puerto Rico, Mayagüez, Puerto Rico, and University of Zululand, KwaDlangezwa, South Africa

Sen Chiao

Department of Meteorology and Climate Science, San Jose State University, San Jose, California

Received 8 November 2010; accepted 2 May 2011

ABSTRACT: The mesoscale structure of the circulation and convection over central Caribbean Antilles islands in midsummer is analyzed. Afternoon thunderstorms are frequent over islands such as Hispaniola and Jamaica as confluent trade winds circulate over heated mountainous topography. Observational data from a rain gauge network, profiles from aircraft and radiosonde, satellite estimates of rainfall, and mesoscale reanalysis fields are studied with a focus on July 2007. A statistical decomposition of 3-hourly high-resolution satellite rainfall reveals an "island mode" with afternoon convection. Trade winds pass over the mountains of Hispaniola and Jamaica with a Froude number <1, leading to a long meandering wake. The Weather Research and Forecasting model is used to simulate climatic conditions during July 2007. The model correctly locates areas of diurnal rainfall that develop because of island heat fluxes, confluent sea breezes, and mountain wakes.

---

* Corresponding author address: Mark R. Jury, Physics Department, University of Puerto Rico, Mayagüez, PR 00681.

E-mail address: mark.jury@upr.edu

DOI: 10.1175/2011EI391.1

KEYWORDS: Caribbean Antilles; Mesoclimate; Jamaica; Mountain wake; Trade wind convection

1. Introduction

The atmospheric boundary layer (ABL) over coasts and large islands often exhibits confluence zones that initiate convective cloud lines (Malkus 1955; Cooper et al. 1982; Blanchard and López 1985; Wilson and Schreiber 1986; Chen and Yu 1988; Wakimoto and Atkins 1994; Kingsmill 1995). The confluence zones involve frictional drag, surface heat fluxes, mountain wakes, and sea breezes—an understanding of which can aid short-range local weather forecasts. The ABL over many tropical islands has been analyzed with regard to circulations driven by diurnal heating (Liu and Moncrieff 1996; Keenan et al. 2000). Large-scale easterly flow is modulated by afternoon sea breezes on the lee side of tropical islands (Carbone et al. 2000). Mountain wakes are narrow, long, and steady under trade wind inversion conditions but wider and turbulent in unstable conditions (Schar and Smith 1993a; Schar and Smith 1993b; Grubisic et al. 1995; Smith et al. 1997). The downstream wake can produce a pair of counterrotating eddies and an associated vorticity dipole. Depending on the Froude and Reynolds numbers and mountain height, either standing waves or drifting vortices can be shed. Wakes and quasi-stationary eddies near mountainous islands are often seen in satellite cloud patterns (Chopra 1973; Etling 1989). Extensive aerial surveys have been conducted around many islands (Smith and Grubisic 1993), and the structure of the trade wind flow has been simulated using mesoscale models for idealized and real conditions (Smith et al. 1997; Burk et al. 2002; Bao et al. 2008).

Among the central Antilles islands of the Caribbean, Hispaniola is 76 000 km^2 and lies upstream in the prevailing trade winds from the Windward Passage and the smaller island of Jamaica (11 000 km^2). Both islands have mountain ranges exceeding 2000-m elevation that are densely vegetated, and sea surface temperatures (SST) over 29°C are common during summer, so the air mass is thermodynamically unstable. These islands are endowed with water resources to support a dense population (3 million in Jamaica and 18 million in Hispaniola, according to 2005 census) because of passing storms and local circulations. Convective clouds tend to form over the highest peaks and drift westward following midday heating, but little is known about the mesoscale processes that organize their development. Our study is motivated by an increasing demand for finescale, accurate short-range (~6 h) forecasts of convection leading to flash floods (Laing 2004). It makes use of the Weather Research and Forecasting model (WRF) in a subtropical setting. Pagowski et al. (Pagowski et al. 2005) evaluated the WRF for its ability to simulate changes in ABL and land surface fluxes under a variety of atmospheric conditions. Research has demonstrated that ABL schemes used in the WRF exhibit scale dependence with respect to diurnal amplitude and weather type (Chiao 2006).

In this study, the primary objectives are as follows: (i) to describe the mesoscale structure of the summer wind field around the central Antilles, (ii) to assess diurnal cycles and ABL structure in flow passing over mountainous vegetated islands, (iii) to understand how the wake of Hispaniola affects the climate of Jamaica, and (iv) to evaluate how a mesoscale model simulates island-scale winds and convection. To achieve these objectives, model reanalyses and simulations are compared with the available observations. There are more than 10 synoptic weather stations that make routine measurements across Hispaniola and Jamaica, and radiosonde profiles are available at the capital cities (Santo Domingo and Kingston). The central Antilles falls within the domain of the National Centers for Environmental Prediction (NCEP) operational 12-km-resolution WRF data assimilation system, thus making it possible to study mesoscale processes underlying trade wind convection over these islands. In section 2, the data and analysis methods are outlined, and section 3 provides the results, which are divided into the regional climatology and case study features. Section 4 is a comparative discussion and summary, with suggestions for further work.

2. Data and analysis methods

The island of Jamaica has a distributed network of 52 rain gauges maintained by the National Meteorological Service. Hourly observations and aircraft profiles are made at regional airports to describe diurnal changes. Radiosonde profiles at Kingston are used to quantify the atmospheric stability and wind shear. These local data are assimilated by NCEP, together with satellite, aircraft, ship, buoy, and ancillary data, to provide the observational density required here. The mesoscale structure of rainfall is quantified using the Climate Prediction Center morphing method (CMORPH) multisatellite product (Joyce et al. 2004) available every 3 h at 25-km resolution. The region's summer mesoclimate is analyzed using the North American Regional Reanalysis (NARR) 32-km 29-level Eta model assimilation (Mesinger et al. 2006), which reflects island-scale winds but has a dry bias over the Antilles islands (Jury 2009). Here, we analyze the mean wind field and diurnal changes in ABL structure for July 2007. This month reflects midsummer conditions: when terrestrial heating is at maximum, trade winds prevail and synoptic disturbances such as westerly troughs and tropical cyclones are infrequent. This month was slightly drier than normal with only three transient easterly waves, so convection was more related to local circulations, the focus of our study. To provide greater detail, the 12-km-resolution operational WRF analyses were considered. National Oceanic and Atmospheric Administration (NOAA) satellite estimates of vegetation fraction [normalized difference vegetation index (NDVI)] and National Aeronautics and Space Administration (NASA) infrared SST fields were analyzed for July 2007.

Three-hourly CMORPH satellite rainfall data for 2007 over a 200 km $\times$ 400 km domain around Jamaica (17°–19.2°N, 79.0°–75.5°W) were subjected to singular value decomposition (SVD). This involves an eigenvector decomposition of the covariance matrix within the rainfall field, so the variability is reduced to modes of descending normalized variance. Each mode has a spatial loading and time scores that describe its fluctuation (Enfield and Alfaro 1999; Chang and Saravanan 2001). The goal here is to distinguish afternoon island-only rainfall from widespread marine rainfall. Mode 5 has a strong diurnal cycle with a focus over the island of Jamaica and negative loading across the surrounding ocean. Its daily averaged time scores correlate at 0.79 with gauge data in July 2007; hence, $\sim$62% of rainfall was locally induced. Cases of trade wind convection over Jamaica were selected by ranking the afternoon mode-5 scores, and 10 days emerge: 7, 17, 18, 19, 20, 21, 22, 24, 27, and 31 July 2007. Aircraft Meteorological Data Relay (AMDAR) wind and temperature reports for case days were analyzed below 1 km at Montego Bay and

Kingston, and composite mean profiles were calculated. Geostationary Operational Environmental Satellite (GOES) infrared images were examined from NASA; Tropical Rainfall Monitoring Mission (TRMM) mean satellite cloud water, ice, and heating profiles were calculated; and *CloudSat* reflectivity slices were obtained for two cases. Statistical analyses were made by correlation of satellite and gauge rainfall with various weather indices drawn from the National Climatic Data Center (NCDC), radiosonde winds, calculated Froude number ($F = U/NH$, where U is the wind speed, N is stability, and H is the mountain height), and operational WRF 850-mb cloud water and 700-mb relative humidity. To briefly study the upper ocean of the central Antilles, Simple Ocean Data Assimilation (SODA) reanalysis fields (Carton and Giese 2008) for July 2007 were analyzed as 1–100-m depth-averaged maps and 1–600-m longitude-averaged vertical sections.

Key aspects of the mean summer climate were simulated using the Advanced Research WRF (ARW-WRF; version 3) over the central Antilles: 15°–22.5°N, 68°–80°W. Our model configuration uses the Yonsei University (YSU) ABL scheme, which permits nonlocal mixing; entrainment of heat, moisture, and momentum; and countergradient transport (Hong and Dudhia 2003) and atmospheric radiation feedbacks (Mlawer et al. 1997). Model precipitation is simulated by grid-scale condensation and convection determined from an explicit moisture scheme that includes ice phase microphysics. The atmospheric component is coupled to the Noah land surface model (Mitchell et al. 2002), which solves the water and energy balance equations (Rogers et al. 2001; Ek et al. 2003; DeHaan et al. 2007). The model was initialized with 3D Global Forecast System (GFS) 0.5°, 3-hourly data from NCEP and run for the month of July 2007. Mean fields were averaged at each phase of the diurnal cycle. The trade winds around Hispaniola and Jamaica affect localized rainfall and ABL structure, which is the focus of our research.

3. Results

3.1. Regional convection, circulation, and coupling

Many studies have documented large-scale summer convection in the Caribbean between May and October that follows the annual cycle of insolation and SST (Malkus 1954; Enfield and Alfaro 1999; Giannini et al. 2000; Chen and Taylor 2002). Although the early and late summer rains derive from westerly troughs and tropical cyclones, the midsummer rains maintain water supplies and agricultural production in the face of high evaporation (Curtis and Gamble 2008; Gamble et al. 2010). Trade winds typically strengthen in July as an anticyclonic ridge extends westward across the North Atlantic (Amador 1998; Jury et al. 2007; Small et al. 2007; Muñoz et al. 2008). Jamaican rainfall observations in July 2007 indicate that 14 days had $\leq$1 mm day^{-1} with a strong ridge present; another 10 days had "beneficial" rain in the range 2–10 mm day^{-1}, the focus of our study; and 3 days had flooding contributed by passing easterly waves. Winds at 925 mb averaged 10 m s^{-1} easterly ($\sigma = 2.2$ m s^{-1}) in July 2007 and, with an ABL lapse rate near moist adiabatic, the Froude number averaged 0.72. The daily 925-mb wind speed was found to be inversely related to 700-mb relative humidity ($r = -0.49$), which in turn affects rainfall ($r = -0.32$), indicating that trade wind subsidence often inhibits convection.

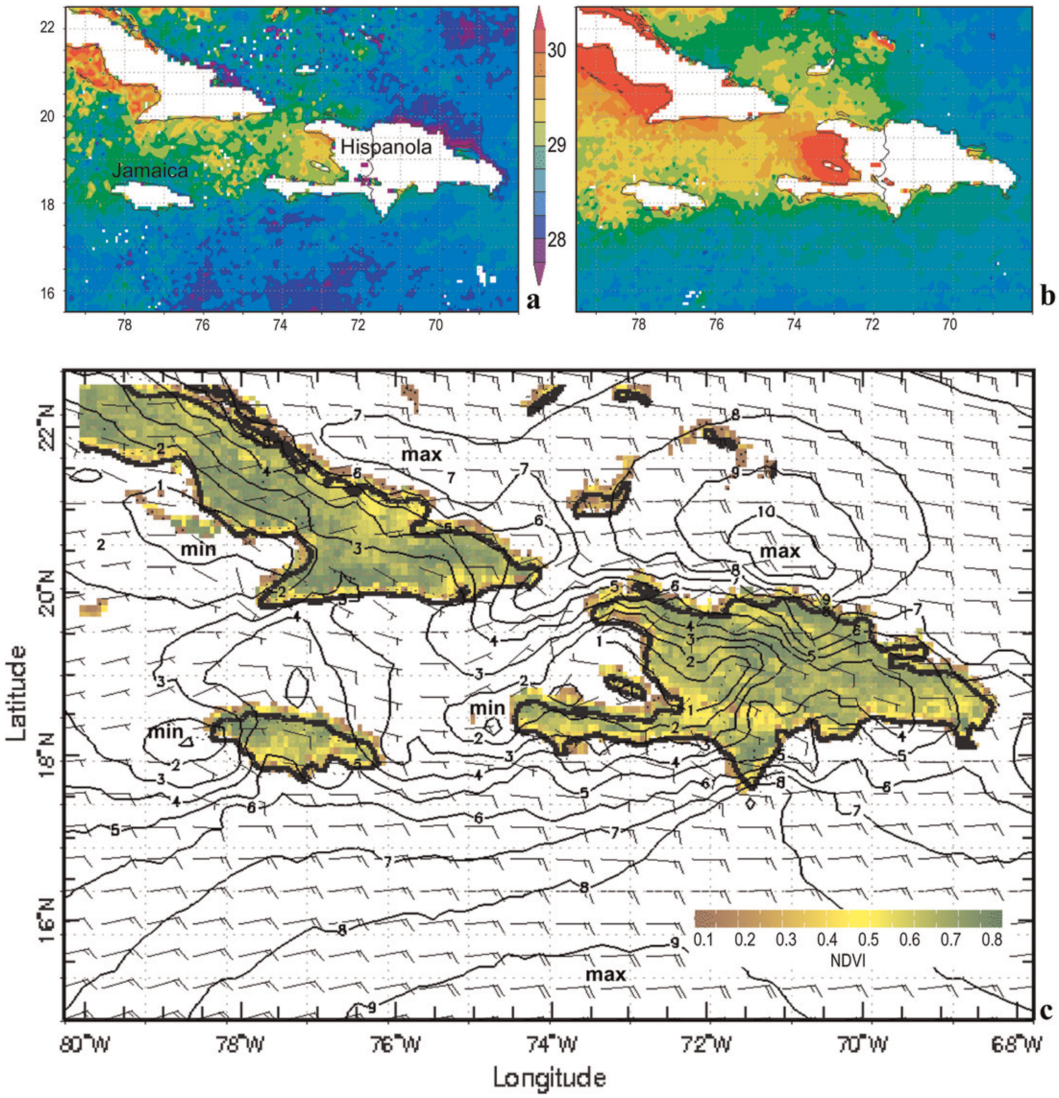

Figure 1. Central Antilles mean NASA SST for (a) nighttime and (b) daytime and (c) satellite vegetation NDVI and NARR surface wind barbs and speed (contours; 1 m s^{-1} interval); all for July 2007.

We analyze the central Antilles SST field for diurnal changes in July 2007 (Figures 1a,b). SSTs at ~28°C are observed across the eastern Caribbean, where evaporative cooling by unobstructed trade winds averages >150 W m^{-2}. The NARR mean surface wind analysis (Figure 1c) exhibits rapid deceleration of trade winds across the central Antilles. In the lee of Hispaniola, there is a band of light winds where afternoon warming induces an SST >30°C. The zone of high SST and calm conditions extends westward between Jamaica and Cuba, so monthly-mean convective available potential energy (CAPE) values exceed 3000 J kg^{-1} (not shown). The SODA reanalysis mean map and section for central Antilles salinity and upper ocean currents is shown in Figures 2a,b. Although Atlantic waters

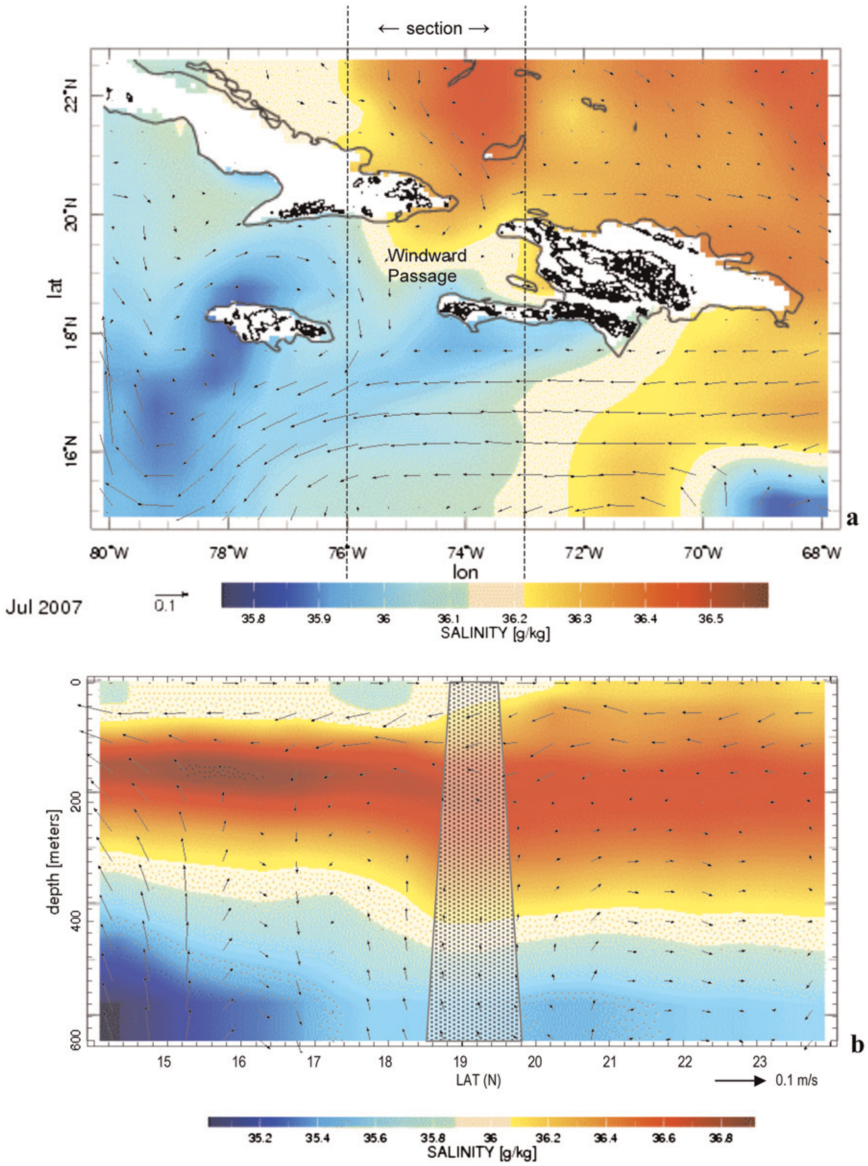

Figure 2. SODA ocean reanalysis July 2007 mean: (a) salinity and currents in the upper 100 m and (b) as north–south depth section averaged over 73°–76°W, illustrating meridional flow. Note that scales vary; elevation > 500 m is contoured in (a); and Hispaniola is shaded in (b).

penetrate the Caribbean passages, enhanced rainfall leeward of Hispaniola induces a low-salinity plume. Ocean currents exhibit a confluence line that extends southwest of Hispaniola, passing Jamaica and inducing anticyclonic rotation there. This draws salty Atlantic waters southward through the Windward Passage at depths of 50–300 m. There is a meridional overturning circulation on the Caribbean side of the Hispaniola wake during July 2007, with freshwater lifting in the zone from 14° to 16°S to join salty southward flow near the surface.

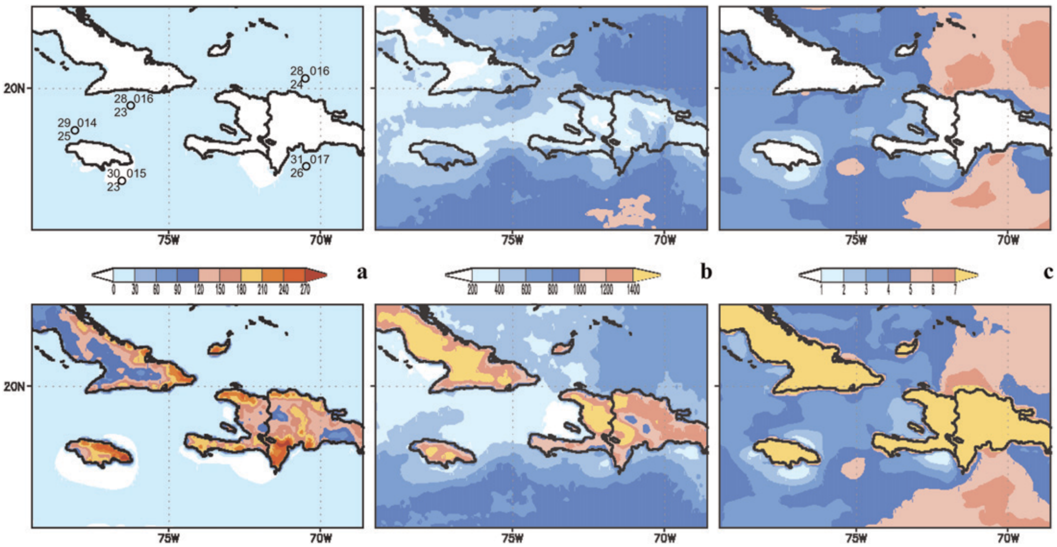

Figure 3. WRF-simulated July 2007 mean: (a) sensible heat flux (W m^{-2}), (b) ABL height (m), and (c) upward moisture flux (mm day^{-1}) at (top) nighttime (0200 LST) and (bottom) daytime (1400 LST). Monthly-mean station plots included in (a).

WRF simulations of surface coupling for different phases of the diurnal cycle in July 2007 are given in Figures 3a–c. At nighttime, there are weak sensible heat fluxes, moderate ABL height, and upward moisture fluxes in the eastern Caribbean zone of strong trade winds. WRF simulations for daytime reveal Antilles island heating with sensible fluxes > 200 W m^{-2}, ABL height > 1400 m, and upward moisture fluxes > 7 mm day^{-1}. Mean coastal station data (Figure 3a) indicate air temperatures in the range 28°–31°C, dewpoints of 23°–26°C, and sea level pressure of 1014–1017 mb decreasing westward. Stations on leeward coasts such as Barahona (18°N, 71°W) tend to be warmer. Unfortunately, there are no observations on the west coast of Hispaniola. The July 2007 rain rate simulated by the WRF is compared with CMORPH satellite estimates for nighttime and daytime periods (Figures 4a,b). There is general agreement at nighttime for the Atlantic and eastern Caribbean rainfall; however, the cloud band associated with the wake of Hispaniola was absent. Daytime convection over the Antilles islands is well simulated with respect to distribution, but intensities were predicted to be higher over mountainous Hispaniola, when satellite estimates show that low-lying Cuba received greater rainfall.

The vertical structure of cloud properties over central Jamaica (Figure 5a) in July 2007 is analyzed from TRMM data in Figure 5b. Monthly-mean cloud latent heating was greatest in the 5–9-km layer near the freezing level, where afternoon thunderstorm updrafts were vigorous. The cloud water content was high in the 2–4-km layer, and there was a dry layer around 6 km. Cloud ice concentrations reach a maximum of ~9 km and were one-third the value of cloud water. Focusing on the diurnal cycle over Jamaica, Atmospheric Infrared Sounder (AIRS) profiles of day minus night specific humidity show a 1–2 g kg^{-1} increase in the 1–5-km layer during a spell of island convection on 18–22 July 2007. Averaged over the entire month,

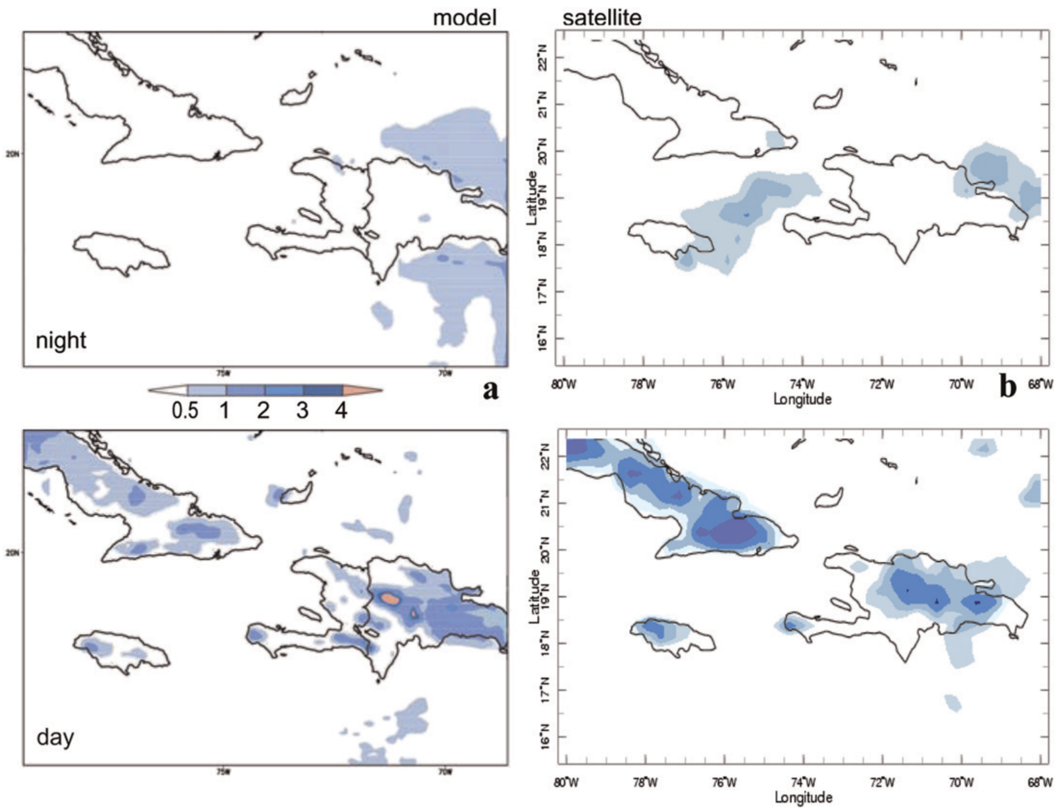

Figure 4. July 2007 mean rain rate (mm day^{-1}): (a) WRF-simulated and (b) CMORPH satellite estimate (top) at nighttime (0200–500 LST) and (bottom) at daytime (1400–1700 LST).

however, daytime values were only 0.5 g kg^{-1} higher in the ABL. We analyze NARR data from 0500 to 1700 LST averaged for July 2007. The time–height section of specific humidity and turbulent kinetic energy (Figure 5d) reveals ABL growth to 2000 m by 1400 LST, consistent with Schafer et al. (Schafer et al. 2001) and Jury et al. (Jury et al. 2009). Sensible heat flux peaks then (Figure 5e), and surface meridional winds converge onto the island with southerly components over the south coast of 4 m s^{-1} by 1700 LST. This indicates the 32-km Eta model assimilation is capable of representing sea-breeze confluence and mountain wakes over Jamaica, similar to Baik (Baik 1992). Although the NARR dry bias inflates daytime sensible fluxes above WRF estimates, its confluent wind circulations are close to observed values.

Island-scale convection was studied by SVD for 3-h rainfall in 2007 ($N = 2920$). The island mode that emerges over the northeastern interior (Figure 6a) has negative loading over the sea with a northeast alignment to the Hispaniola wake. SVD scores averaged over the diurnal cycle (Figure 6b) reveal a peak during the afternoon at 1400–1700 LST, as found over Puerto Rico by Carter and Elsner (Carter and Elsner 1997) and Jury et al. (Jury et al. 2009). Marine convection contributed by passing troughs and waves tends to peak from 0200 to 0800 LST and has little diurnal amplitude (not shown). The variance explained by the marine mode is 32%

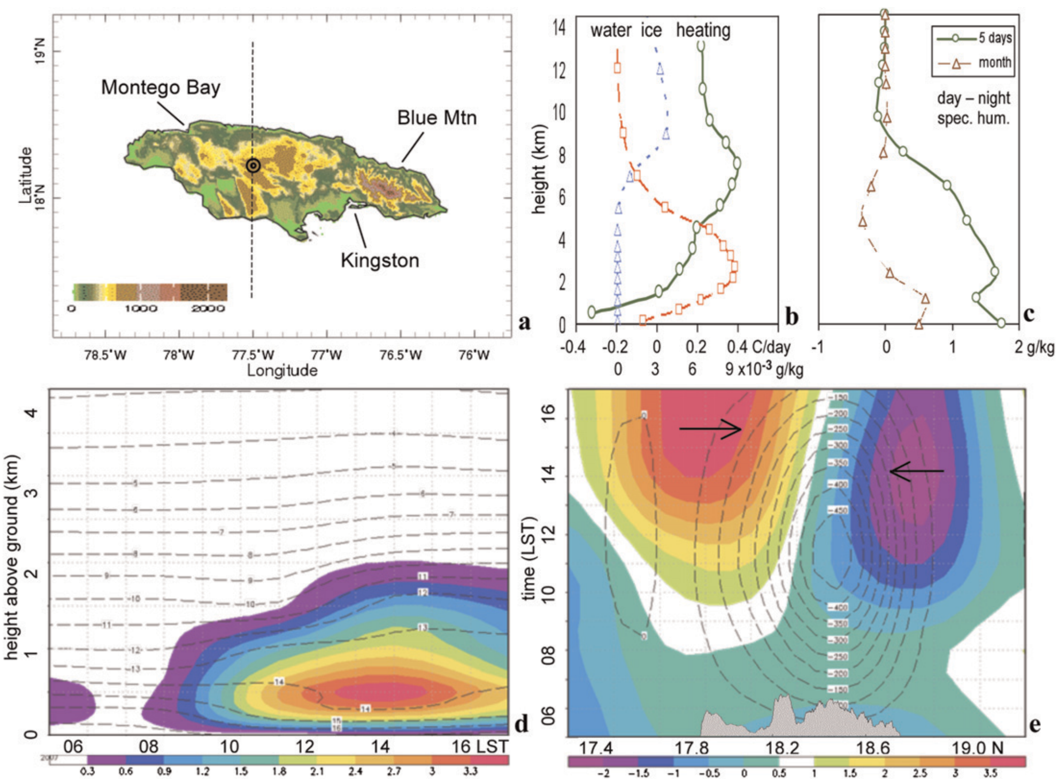

Figure 5. (a) Jamaica topography and place names. (b) July 2007 TRMM profiles of cloud water, ice, and latent heating. (c) AIRS profiles of monthly- and 5-day-mean day minus night differences in specific humidity, at dot in (a). NARR July 2007 mean: (d) time–height section of specific humidity (dashed) and turbulent kinetic energy at dot in (a) and (e) latitude–time section of sensible heat flux (dashed) and surface meridional wind component on line in (a).

compared with 10% for the island mode. Our analysis uses the afternoon SVD scores (Figure 6c) to identify cases of rainfall over Jamaica: 7, 17, 18, 19, 20, 21, 22, 24, 27, and 31 July 2007. CMORPH satellite rain estimates and gauge data are in good agreement in midsummer (Figure 6d): the mean correlation is 0.61 (N = 124). At low (high) rain rates, the satellite underestimates (overestimates) the island average.

3.2. Case study features

Three-hourly values of 850-mb cloud water and 700-mb relative humidity from the operational WRF are illustrated in Figure 7a. They tend to oscillate with the passage of easterly waves and rose in the third week of July 2007. We analyze vertical sections of AIRS relative humidity and NCEP wind circulations in the period 18–22 July (Figures 7c,d). A zonal overturning is evident: sinking motion in the low-level easterlies near Hispaniola contrasts with rising motion joining the

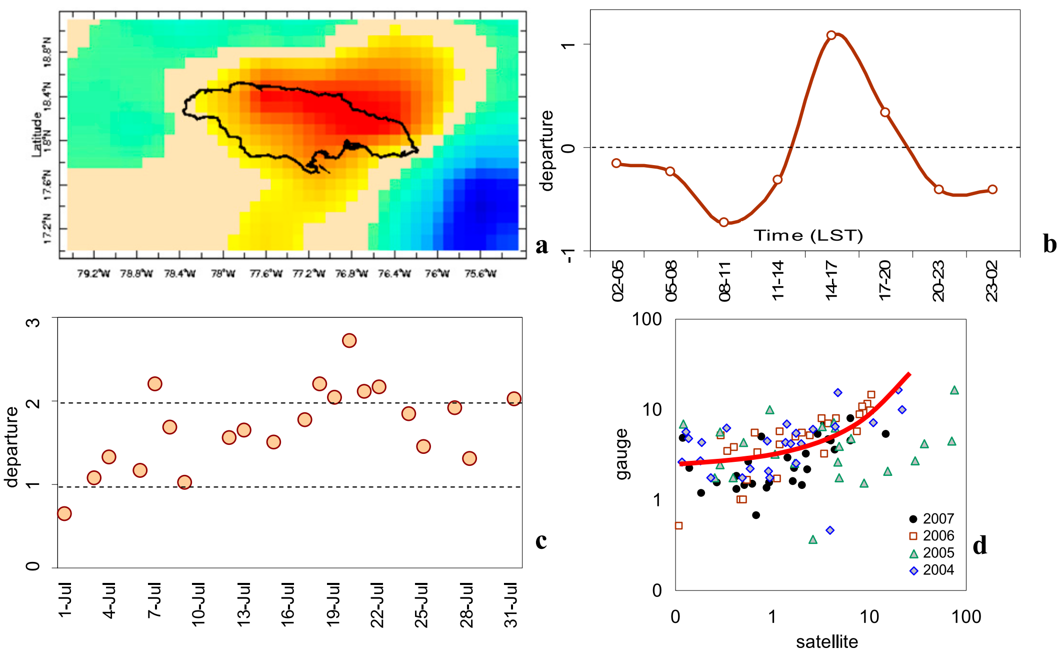

Figure 6. CMORPH 3-h rainfall SVD mode-5 (a) spatial loading pattern, (b) diurnally averaged time scores, and (c) afternoon time scores in 2007 used for case selection. (d) Satellite vs gauge log-scale scatterplot of daily rainfall (mm) over Jamaica each July for 2004–07 with mean second-order trend (red).

upper westerlies over Jamaica. The humidity structure has the expected high values near the surface and a dry layer above 500 mb that slopes down toward the west and dissipates near Jamaica. The meridional slice indicates a weak overturning in the low levels but a rising southerly flow above 300 mb. The low-level humidity deepens to the north and connects to an upper moist layer over Jamaica. There is a dry layer around 500 mb that penetrates from the Caribbean.

CloudSat vertical slices of water/ice reflectivity on two case days are given in Figures 8a,b. The north–south section for 19 July is over Hispaniola at 1400 LST. The main axis of convection was over the Caribbean coast, where sea-breeze-modified trade winds "wrap" onto the island. The highest reflectivity values were in the 3–8-km layer in a thunderstorm ~20 km wide. There was decreasing convection in bands over the Cordillera Central and over the Atlantic coast. At 1400 LST 24 July, convection was deeper, with high cloud water/ice reflectivity values in the 3–10-km layer. Bands of convection were located over Jamaica's Caribbean coast, in the central Windward Passage with the Hispaniola wake, and over Cuba. Tower widths were <20 km over Jamaica and Cuba but exceeded 40 km around 18.7°N, suggesting a twin wake structure with more vigorous convection in the southern cell. The bands of convection tilt poleward at ~10 km with height because of upper winds. The vertical structure of meridional overturning from NCEP reanalysis is overlaid on the cloud reflectivity slices (Figures 8a,b). At 1400 LST 19 July, the flow rose over Hispaniola and turned equatorward in midlevels. There was a subsident layer around 9 km and poleward flow aloft. The circulation on 24 July

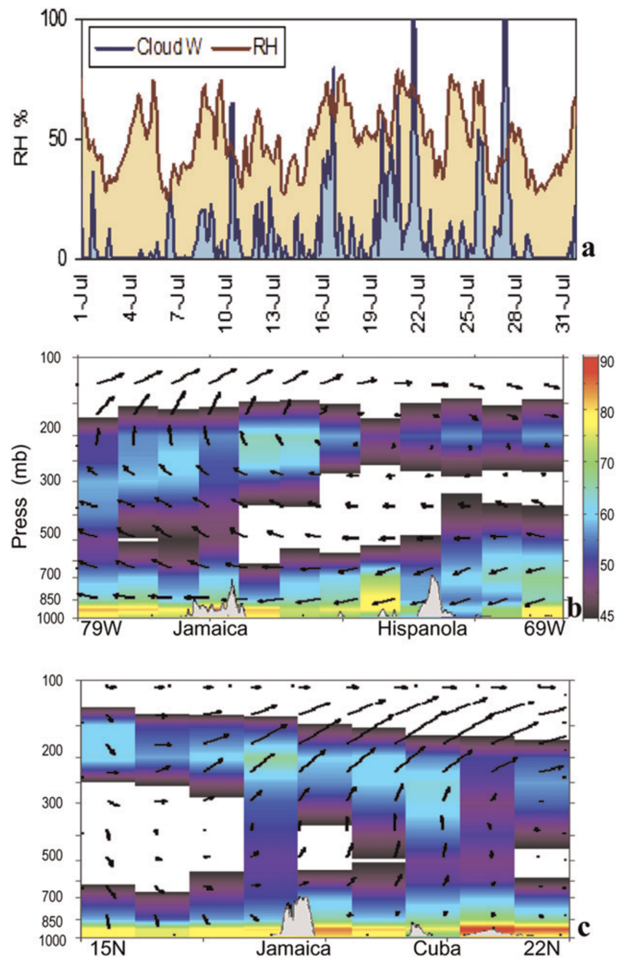

Figure 7. (a) Three-hourly time series of operational WRF 700-mb relative humidity and 850-mb cloud water over central Jamaica. AIRS satellite relative humidity, NCEP wind, and vertical motion averaged over 18–22 Jul 2007 along a vertical section (b) east–west and (c) north–south over Jamaica. Largest vector in (b) is 10 m s^{-1}, largest vector in (c) is 5 m s^{-1}, and vertical motion is exaggerated 30-fold.

was somewhat different. The meridional overturning was more pronounced: near-surface flow was poleward; upper flow was equatorward; and sinking and rising limbs were located over 17° and 20°N, respectively. WRF 10-m wind vorticity is analyzed across the *CloudSat* sections. There are anticyclonic (cyclonic) pairs associated with Hispaniola, Jamaica, and Cuba that reflect accelerated trade winds on south (north) coasts. Convection tends to occur on these confluent shear lines, in agreement with the modeling studies of Chu and Lin (Chu and Lin 2000).

Composite mean afternoon AMDAR profiles within the 1-km ABL at Montego Bay and Kingston are compared in Figures 9a–c. Mean wind directions on the leeward coast (Montego) are easterly throughout the ABL. On 30% of case days, a 250-m-deep, 3 m s^{-1} westerly sea breeze prevails there. On the Caribbean coast

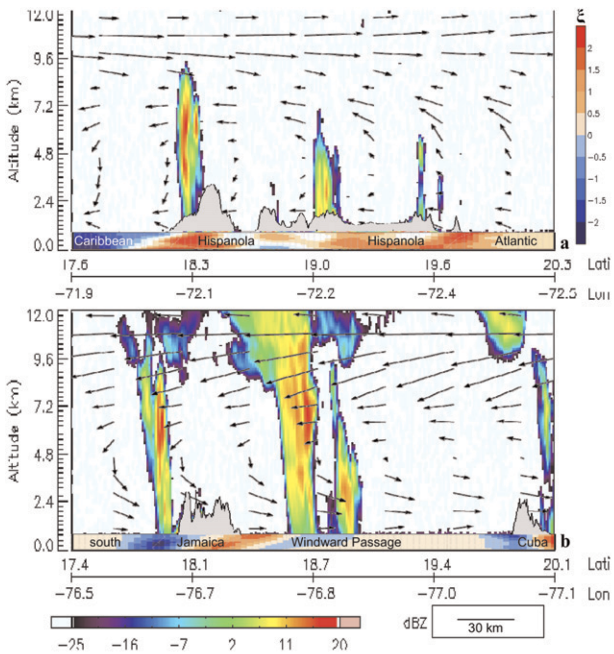

Figure 8. ***CloudSat*** **vertical slices on (a) 19 and (b) 24 Jul 2007 with terrain profiles and NCEP meridional flow (largest vector 5 m s^{-1}) with vertical motion exaggerated 30-fold. Surface horizontal bars are WRF wind vorticity with scale shown at top right × 10^{-5} s^{-1}.**

(Kingston), near-surface winds are at ~130° and gradually swing easterly with height. The confluent angle is thus 40°. The wind speed profile at Kingston exhibits a jet structure >7 m s^{-1} in the 100–300-m layer, declining to 5 m s^{-1} in the upper ABL. Montego Bay, being leeward, experiences mean winds below 400 m that are

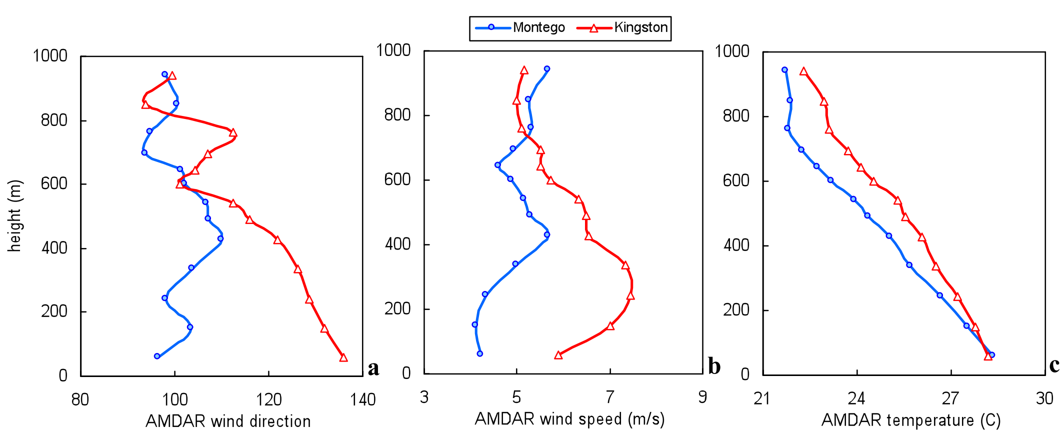

Figure 9. Composite ~1500 LST AMDAR profiles at Montego Bay and Kingston averaged over 10 case days in July 2007: (a) wind direction, (b) wind speed, and (c) temperature.

3 m s^{-1} less. The surface heating and frictional drag that slow the trade winds crossing Jamaica produce low-level moisture convergence. The lapse rate at Montego Bay is 2°C steeper than Kingston below 800 m, reflecting an air mass that has been modified by island evapotranspiration and warmer SST in the Windward Passage north of the island (cf. Figure 1b). The Caribbean air mass, on the other hand, is more subsident and SSTs are 1°C cooler there. The composite mean temperature profiles both exhibit a weak inversion in the 800–900-m layer.

Time series of operational North American Mesoscale (NAM) model surface heat fluxes and CAPE over central Jamaica (cf. Figure 6a) in the period 18–20 July 2007 are given in Figure 10a. The surface sensible and latent fluxes peaked near 200 W m^{-2} from 1100 to 1400 LST, whereas CAPE exceeded 3000 J kg^{-1} from 1400 to 1700 LST. A maximum daily rainfall of 130 mm was reported on 19 July. A back-trajectory analysis for that day (Figure 10b) reveals that low-level inflow derived from the Windward Passage and northern Hispaniola. A similar analysis for a second case day (31 July) exhibited low-level inflow from the Caribbean south of Hispaniola. Surprisingly, flow from the northeast (19 July) had a rising tendency, whereas flow on the 31 July was more subsident. The 10-m absolute vorticity field from the operational WRF (Figures 10c,d) exhibits dipole patterns extending downstream from the Antilles islands at 1400 LST 19 and 31 July 2007. The Hispaniola wake tends to align and merge with the shear line over Jamaica. The Kingston radiosonde profiles for the case study days (Figures 10e,f) exhibit similar thermodynamic conditions: deep moisture, unstable lapse rate, and no subsidence inversion. The two cases differ in their wind profile: 19 July had weak trade winds and upper southerlies, whereas 31 July had deep easterly flow.

An hourly sequence of GOES infrared images during the afternoon of 31 July 2007 is given in Figures 11a–d. Convection first developed over the ~2000-m Blue Mountains of Jamaica by 1300 LST, the time of peak surface heating. At 1400 LST, the cloud band spread westward across the island at 10 m s^{-1}. By 1600 LST, convection had expanded horizontally into a circular thunderstorm of ~100-km diameter with cloud tops of −70°C (~14 km), producing a maximum rainfall of 60 mm. The WRF wind field (Figure 11e) exhibits northeasterly trade winds that accelerate around the island reaching speeds of 14 kt some 40 km off Kingston and Montego Bay. Mountain wakes from Hispaniola and Jamaica are clearly evident with outgoing/incoming speeds of 2–4 kt that connect across the island and draw airflow toward the thunderstorm. In contrast, lower-resolution Eta and GFS model reanalyses have a more easterly surface wind field (not shown). AMDAR winds at Montego Bay are in agreement with the WRF analysis. However, at Kingston, model winds do not wrap sufficiently onto the coast (80°) compared with aircraft (130°), suggesting problems in handling the sea breeze and Ekman spiral.

4. Discussion and summary

Our objective was to evaluate changes in surface fluxes, ABL height, and sea-breeze-modified trade winds as they contribute to diurnal convection in the central Antilles region. The WRF simulates a shallow homogeneous ABL of ~300 m during the night and a daytime increase of >1400 m over the islands. Kinematic wakes form behind Hispaniola's 3000-m Cordillera Central and Jamaica's Blue Mountains. Shear lines form between trade winds of Atlantic and Caribbean origin

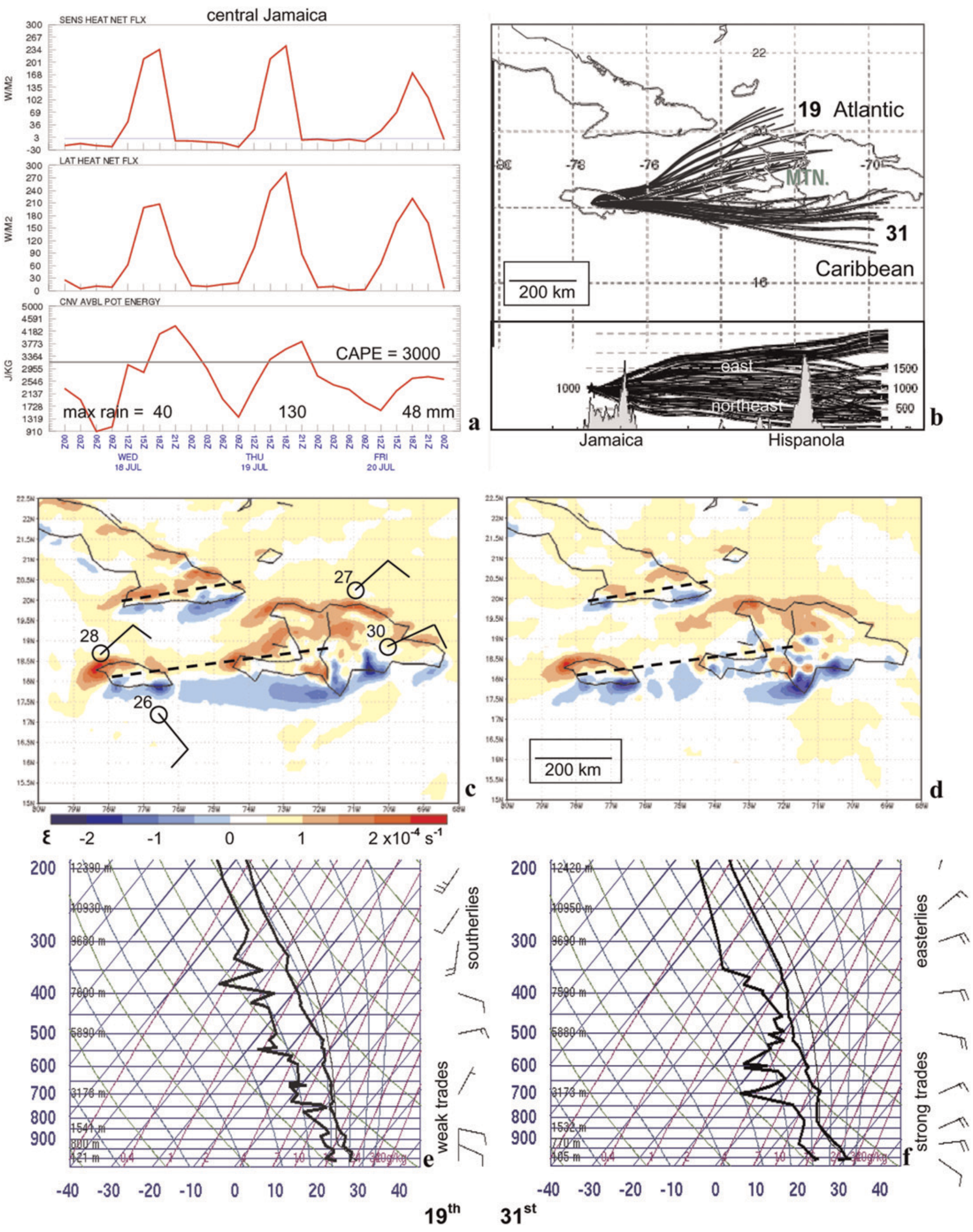

Figure 10. (a) Operational WRF-assimilated meteogram for central Jamaica 18–20 Jul 2007 when island convection prevailed. (b) Hybrid Single-Particle Lagrangian Integrated Trajectories (HYSPLIT) model GFS ensemble back trajectories for 24-h periods ending 1700 LST 19 and 31 Jul 2007, with vertical section lower. WRF 10-m absolute vorticity at 1400 LST on (c) 19 and (d) 31 Jul 2007. Dashed line is island wake. (e),(f) Kingston radiosonde profiles for same days. The 100-m AMDAR reports are included in (c).

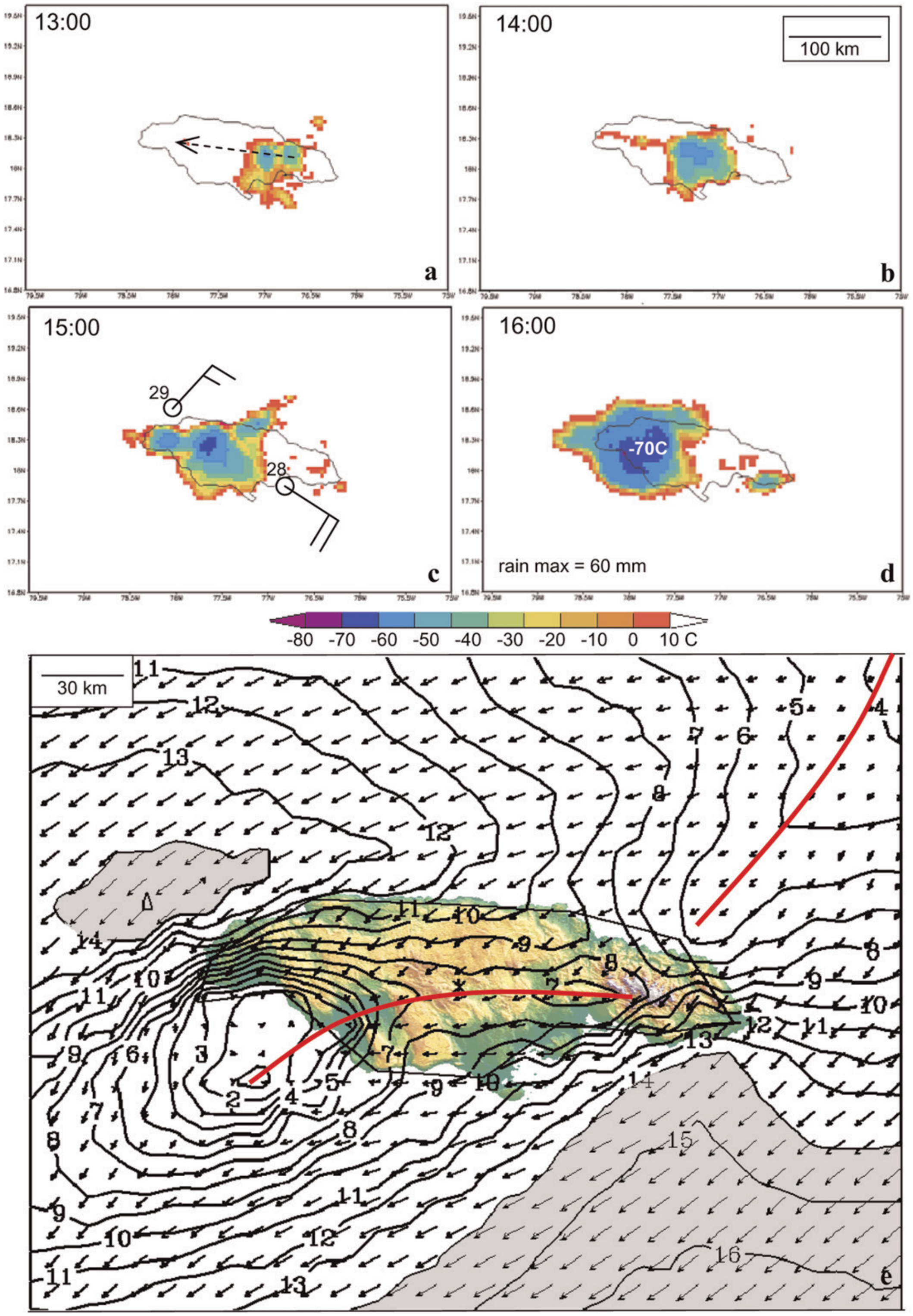

Figure 11. (a)–(d) Hourly sequence of GOES infrared images for 1300–1600 LST 31 Jul 2007. Arrow reflects cell movement in (a), and 100-m AMDAR wind and temperature are shown in (c). (e) WRF 10-m wind and speed contours (kt) at 1400 LST with topography shaded. Red lines are calm wakes, and gray shading denotes >14 kt.

and SSTs exceed 30°C west of Hispaniola. Daytime heating turns the trade winds 20°–30° onshore along the north and south coasts, so moist unstable air converges over the western half of the islands during afternoon. Rain shadow zones develop along the southern flank of the islands of Hispaniola and Jamaica (cf. Figure 4; Gamble and Curtis 2008). Topographic flow interactions are characterized by a Froude number <1, so Antilles mountain wakes extend downstream as in the Hawaiian Islands (Burk et al. 2002) but with a weaker inversion above the ABL. The wind confluence lines are enriched by evapotranspiration fluxes during the afternoon, so CAPE rises above 3000 J kg^{-1}. The direction of flow is critical: easterly winds provide the longest over-island fetch. Surface heat fluxes estimated by the WRF reach 300 W m^{-2} over Jamaica, but no direct observations are available for comparison.

The upper ocean fields clearly reflect a wake from Hispaniola, with lower salinity and confluent westward currents. This zone experiences significant diurnal heating, so SSTs there rise above 30°C in an axis that extends westward to the south of Cuba, forming the leading edge of the "warm pool." Because of salty poleward flow through the Windward Passage, the oceanic wake deviates south of Jamaica, producing a large anticyclonic rotor there in July 2007. In the Caribbean sector, there is upward vertical motion that joins poleward currents near the surface.

The climate of the central Antilles was studied using existing data and model-analyzed fields, with a focus on the diurnal cycle and its mesoscale features in midsummer trade wind conditions. Daytime surface heating creates a thermal low over the western plains of the central Antilles islands. NARR fields for July 2007 exhibit air temperatures up to 37°C over western Hispaniola and a thermal low of 1015.5 mb. A landward pressure gradient of 2 mb $(100\ \mathrm{km})^{-1}$ causes an infolding of trade winds from the north and south coasts. By early afternoon, confluent shear lines develop over the islands of Hispaniola and Jamaica. The summer air mass is moist, dewpoint temperature Td ~24°C, and unstable, T ~30°C, and afternoon thunderstorms form along the shear lines and drift westward bringing rainfall ~10 mm h^{-1}. By sunset, the thunderstorms collapse and thermal lows weaken, allowing trade winds to resume. During the night, radiatively cooled air drains from the mountains and joins the trade winds, enhancing marine convection.

This study has described variations of the ABL across the central Antilles based on limited in situ data, mesoscale reanalysis, and model simulations. The ability of the WRF to generate wind confluence, ABL response to surface heating, and convective rainfall were evaluated with a view to improved short-range weather forecasting. The model simulated the development of afternoon thunderstorms over the islands but did not maintain nocturnal convection in the Hispaniola wake. Further idealized WRF experiments may help distinguish the kinematic and thermodynamic effects. Although some verification data from an expanding network of automatic weather stations is anticipated, information on the vertical structure of circulations is limited. In that regard, aerial surveys, flux towers, and Doppler weather radar would aid our understanding. Then model sensitivity studies could better isolate the influences of sea breeze, orography, and evapotranspiration.

Acknowledgments. We acknowledge the data suppliers (http://ingrid.ldgo.columbia.edu; http://nomads.ncdc.noaa.gov/; http://disc.sci.gsfc.nasa.gov/giovanni; http://ready.arl.noaa.gov;

http://amdar.noaa.gov; http://weather.uwyo.edu/upperair/). L. Brown of the Jamaican NMS kindly provided rain gauge data. Computations were performed at the National Center for Atmospheric Research. The second author is supported by the National Science Foundation Grant AGS-0855286.

References

Amador, J. A., 1998: A climatic feature of the tropical Americas: The trade wind easterly jet. *Topicos Meteorologicos Oceanograficos,* **5,** 1–13.

Baik, J. J., 1992: Response of a stably stratified atmosphere to low-level heating: An application to the heat island problem. *J. Appl. Meteor.,* **31,** 291–303.

Bao, J.-W., S. A. Michelson, P. O. G. Persson, I. V. Djalalova, and J. M. Wilczak, 2008: Observed and WRF-simulated low-level winds in a high-ozone episode during the Central California Ozone Study. *J. Appl. Meteor. Climatol.,* **47,** 2372–2394.

Blanchard, D. O., and R. E. López, 1985: Spatial patterns of convection in south Florida. *Mon. Wea. Rev.,* **113,** 1282–1299.

Burk, S. D., T. Haack, L. T. Rogers, and L. J. Wagner, 2002: Island wake dynamics and wake influence on the evaporation duct and radar propagation. *J. Appl. Meteor.,* **42,** 349–367.

Carbone, R. E., J. W. Wilson, T. D. Keenan, and J. M. Hacker, 2000: Tropical island convection in the absence of significant topography. Part I: Life cycle of diurnally forced convection. *Mon. Wea. Rev.,* **128,** 3459–3480.

Carter, M. M., and J. B. Elsner, 1997: A statistical method for forecasting rainfall over Puerto Rico. *Wea. Forecasting,* **12,** 515–525.

Carton, J. A., and B. S. Giese, 2008: A reanalysis of ocean climate using Simple Ocean Data Assimilation (SODA). *Mon. Wea. Rev.,* **136,** 2999–3017.

Chang, P., and R. Saravanan, 2001: A hybrid coupled model study of tropical Atlantic variability. *J. Climate,* **14,** 361–390.

Chen, A. A., and M. Taylor, 2002: Investigating the link between early season Caribbean rainfall and the El Niño + 1 year. *Int. J. Climatol.,* **22,** 87–106.

Chen, G. T.-J., and C.-C. Yu, 1988: Study of low-level jet and extremely heavy rainfall over northern Taiwan in the mei-yu season. *Mon. Wea. Rev.,* **116,** 884–891.

Chiao, S., 2006: Performance of planetary boundary layer schemes in the WRF model. *Proc. 25th Army Science Conf.,* Orlando, FL, U.S. Army, XX–XX.

Chopra, K. P., 1973: Atmospheric and oceanic flow problems introduced by islands. *Advances in Geophysics,* Vol. 16, Academic Press, 298–416.

Chu, C.-M., and Y.-L. Lin, 2000: Effects of orography on the generation and propagation of mesoscale convective systems in a two-dimensional conditionally unstable flow. *J. Atmos. Sci.,* **57,** 3817–3837.

Cooper, H., M. Garstang, and J. Simpson, 1982: The diurnal interaction between convection and peninsular-scale forcing over south Florida. *Mon. Wea. Rev.,* **110,** 486–503.

Curtis, S., and D. W. Gamble, 2008: Regional variations of the Caribbean mid-summer drought. *Theor. Appl. Climatol.,* **94,** 25–34.

De Haan, L. L., M. Kanamitsu, C. H. Lu, and J. O. Roads, 2007: A comparison of the Noah and OSU land surface models in the ECPC seasonal forecast model. *J. Hydrometeor.,* **8,** 1031–1048.

Ek, M. B., K. E. Mitchell, Y. Lin, R. Rogers, P. Grunmann, V. Koren, G. Gayno, and J. D. Tarpley, 2003: Implementation of Noah land surface model advances in the National Centers for Environmental Prediction operational mesoscale ETA model. *J. Geophys. Res.,* **108,** 8851, doi:10.1029/2002JD003296.

Enfield, D. B., and E. J. Alfaro, 1999: The dependence of Caribbean rainfall on the interaction of the tropical Atlantic and Pacific Oceans. *J. Climate,* **12,** 2093–2103.

Etling, D., 1989: On atmospheric vortex streets in the wake of large islands. *Meteor. Atmos. Phys.,* **41,** 157–164.

Gamble, D. W., and S. Curtis, 2008: Caribbean precipitation: Review, model, and prospect. *Prog. Phys. Geogr.,* **23,** 265–276.

——, D. Campbell, T. Allen, D. Barker, S. Curtis, D. McGregor, and J. Popke, 2010: Climate change, drought, and Jamaican agriculture: Local knowledge and the climate record. *Ann. Assoc. Amer. Geogr.,* **100,** 880–893.

Giannini, A., Y. Kushnir, and M. A. Cane, 2000: Interannual variability of Caribbean rainfall, ENSO, and the Atlantic Ocean. *J. Climate,* **13,** 297–311.

Grubisic, V., R. B. Smith, and C. Schar, 1995: The effect of bottom friction on shallow-water flow past an isolated obstacle. *J. Atmos. Sci.,* **52,** 1985–2005.

Hong, S.-Y., and J. Dudhia, 2003: Testing of a non-local boundary layer vertical diffusion scheme in numerical weather prediction applications. Preprints, *20th Conf. Weather Analysis and Forecasting,* Seattle, WA, Amer. Meteor. Soc., 17.3. [Available online at http://ams.confex.com/ams/pdfpapers/72744.pdf.]

Joyce, R. J., J. E. Janowiak, P. A. Arkin, and P. Xie, 2004: CMORPH: A method that produces global precipitation estimates from passive microwave and infrared data at high spatial and temporal resolution. *J. Hydrometeor.,* **5,** 487–503.

Jury, M. R., 2009: An intercomparison of observational, reanalysis, satellite, and coupled model data on mean rainfall in the Caribbean. *J. Hydrometeor.,* **10,** 413–430.

——, B. A. Malmgren, and A. Winter, 2007: Sub-regional precipitation climate of the Caribbean and relationships with ENSO and NAO. *J. Geophys. Res.,* **112,** D16107, doi:10.1029/2006JD007541.

——, S. Chiao, and E. W. Harmsen, 2009: Mesoscale structure of trade wind convection over Puerto Rico, composite observations and numerical model simulation. *Bound.-Layer Meteor.,* **132,** 289–313.

Keenan, T. D., and Coauthors, 2000: The Maritime Continent Thunderstorm Experiment (MCTEX): Overview and results. *Bull. Amer. Meteor. Soc.,* **81,** 2433–2455.

Kingsmill, D. E., 1995: Convection initiation associated with a sea-breeze front, a gust front, and their interaction. *Mon. Wea. Rev.,* **123,** 2913–2933.

Laing, A. G., 2004: Cases of heavy precipitation and flash floods in the Caribbean during El Niño winters. *J. Hydrometeor.,* **5,** 577–594.

Liu, C., and M. W. Moncrieff, 1996: A numerical study of the effects of ambient flow and shear on density currents. *Mon. Wea. Rev.,* **124,** 2282–2303.

Malkus, J. S., 1954: Some results of a trade cumulus cloud investigation. *J. Meteor.,* **11,** 220–237.

——, 1955: The effects of a large island upon the trade-wind air stream. *Quart. J. Roy. Meteor. Soc.,* **81,** 538–550.

Mesinger, F., and Coauthors, 2006: North American Regional Reanalysis. *Bull. Amer. Meteor. Soc.,* **87,** 343–360.

Mitchell, K. E., and Coauthors, 2002: The community Noah land surface model (LSM) user's guide. NOAA Rep.

Mlawer, E. J., S. J. Taubman, P. D. Brown, M. J. Iacono, and S. A. Clough, 1997: Radiative transfer for inhomogeneous atmosphere: RRTM, a validated correlated-k model for the long-wave. *J. Geophys. Res.,* **102** (D14), 16 663–16 682.

Muñoz, E., A. J. Busalacchi, S. Nigam, and A. Ruiz-Barradas, 2008: Winter and summer structure of the Caribbean low-level jet. *J. Climate,* **21,** 1260–1276.

Pagowski, M., J. Hacker, J. W. Bao, 2005: Behaviour of WRF PBL schemes and land-surface models in 1-D simulation during BAMEX. *Proc. WRF Users Workshop,* Boulder, CO, National Center for Atmospheric Research, 27–30.

Rogers, E., M. Ek, Y. Lin, K. Mitchell, D. Parrish, and G. DiMego, 2001: Changes to the NCEP Meso ETA analysis and forecast system: Assimilation of observed precipitation, land-surface physics, modified 3-D VAR analysis. NOAA Rep. [Available online at http://www.emc.ncep.noaa.gov/mmb/mmbpll/spring2001/tpb/.]

Schafer, R., P. T. May, T. D. Keenan, K. McGuffie, W. L. Ecklund, P. E. Johnston, and K. S. Gage, 2001: Boundary layer development over a tropical island during the Maritime Continent Thunderstorm Experiment. *J. Atmos. Sci.,* **58,** 2163–2179.

Schar, C., and R. B. Smith, 1993a: Shallow-water flow past isolated topography. Part I: Vorticity production and wake formation. *J. Atmos. Sci.,* **50,** 1373–1400.

——, and ——, 1993b: Shallow-water flow past isolated topography. Part II: Transition to vortex shedding. *J. Atmos. Sci.,* **50,** 1401–1412.

Small, R. J. O., S. P. de Szoeke, and S. P. Xie, 2007: The Central American mid-summer drought: Regional aspects and large-scale forcing. *J. Climate,* **20,** 4853–4873.

Smith, R. B., and V. Grubisic, 1993: Aerial observations of Hawaii's wake. *J. Atmos. Sci.,* **50,** 3728–3750.

——, A. C. Gleason, P. A. Gluhosky, and V. Grubisic, 1997: The wake of St. Vincent. *J. Atmos. Sci.,* **54,** 606–623.

Wakimoto, R. M., and N. T. Atkins, 1994: Observations of the sea-breeze front during CaPE. Part I: Single-Doppler, satellite, and cloud photogrammetry analysis. *Mon. Wea. Rev.,* **122,** 1092–1114.

Wilson, J. W., and W. E. Schreiber, 1986: Initiation of convective storms at radar-observed boundary-layer convergence lines. *Mon. Wea. Rev.,* **114,** 2516–2536.